Influence of the Surface Texture Parameters of Asphalt Pavement on Light Reflection Characteristics

Peng Xu *, Guoping Qian, Chao Zhang, Xiangdong Wang, Huanan Yu, Hongyu Zhou, Chen Zhao

Posted Date: 24 October 2023

doi: 10.20944/preprints202310.1535.v1

Keywords: macro-micro texture; retroreflection coefficient; rutting test; single factor model; quadratic function; multifactor model

Article

Influence of the Surface Texture Parameters of Asphalt Pavement on Light Reflection Characteristics

Peng Xu [1,2,*], Guoping Qian [2], Chao Zhang [2], Xiangdong Wang [2], Huanan Yu [2], Hongyu Zhou [2] and Chen Zhao [2]

[1] Hunan Key Laboratory of Smart Roadway and Cooperative Vehicle-Infrastructure Systems, Changsha University of Science & Technology, Changsha 410114, China
[2] School of Traffic and Transportation Engineering, Changsha University of Science & Technology, Changsha 410114, China
* Correspondence: xupeng@csust.edu.cn

Abstract: The optical reflection characteristics of asphalt pavement are an important influencing factor in road lighting design, and the macro and micro textures of asphalt pavement significantly affect its reflection characteristics. To investigate the impact of texture parameters on the retroreflection coefficient of asphalt pavement, this study obtained the macroscopic and microscopic texture properties of rutting board specimens and on-site asphalt pavement using a pavement texture tester. The macro- and microtexture parameters, such as macroscopic texture distribution density (D_1), microscopic texture distribution density (D_2), profile height root-mean-square (R_q), profile slope root-mean-square (Δq), skewness R_{sk} and kurtosis R_{ku}, were measured, and the corresponding retroreflection coefficient R_L was measured using a retro-reflectometer. In the laboratory experiments, rutting specimens of AC-13, SMA-13, and OGFC-13 asphalt mixtures were formed. The changes in texture parameters and retroreflection coefficient of different rutting specimens before and after crushing were studied, and a factor influence model between macro- and microtexture parameters and R_L was established. And the correlation models of texture index and R_L of asphalt pavement are further established. The results showed that in the single factor model, the parameters can be used to characterize R_L with high prediction accuracy, whereas for the on-site measurements, the three parameters of Δq, Rsk, and Rku can characterize the R_L well. The nonlinear model established on the basis of the B-P neural network algorithm improves its prediction accuracy. This research can provide ideas for optimizing the reflection characteristics of asphalt pavement and further provide a decision-making basis for road lighting design.

Keywords: macro-micro texture; retroreflection coefficient; rutting test; single factor model; quadratic function; multifactor model

1. Introduction

Scientific and reasonable road lighting is important for improving road safety [1–3] and reducing energy consumption [4]. The optical reflection characteristics of road surface is one of the important bases for road lighting calculation, and the International Lighting Association CIE recommends the use of reduced brightness coefficient table (r-table) to represent the reflection characteristics of different paving materials and gives some columns of standard r-table [5], which is used in all kinds of lighting design software calculations, and it provides a great convenience for the design work of road lighting. However, the standard r-tables obtained based on the measurement data in the 1970s do not widely represent the reflectance characteristics of the actual roads today, and the use of the uncorrected r-tables for lighting design will lead to the deviation between the designed and actual brightness of the pavement [6]. In recent years, more and more research efforts have been devoted to obtaining the reduced brightness coefficient tables representing the actual road reflectance characteristics [7–11] or developing various types of test devices for accurately obtaining road reflectance characteristics [12–14], to accurately obtain the optical reflectance characteristics of the actual road and improve the accuracy of road lighting design.

However, accurately obtaining data in the form of reduced luminance coefficient requires a lot of cumbersome laboratory measurements, and the instruments to carry out the relevant

 doi:10.20944/preprints202310.1535.v1

measurements in the road site have not yet been popularized, and are more in the experimental stage, so the International Illuminating Association, CIE, recommends the use of retro-reflectivity coefficient RL, which is measured in the road site, to indicate the reflective characteristics of the pavement surface [5].

Pavement surface texture is defined as the deviation of the pavement surface from the true plane [15]. The International Road Association (PIARC) [16] classified the surface structure of asphalt pavements into four types: micro-texture, macro-texture, macrostructure and unevenness, based on the wavelength in the horizontal direction, the amplitude in the vertical direction, the power spectral characteristics of asphalt pavements, and their possible impact on road users, where the micro-texture is less than 0.5 mm, and the macro-texture is between 0.5-50.0 mm range [17]. The pavement texture depends on the composition of the top layer of the pavement material, while the reflectivity of the surface is determined by the micro- and macro-textures [18].

Macrotexture refers to the irregularities in the rough texture of the road surface and these irregularities are mainly dependent on the nature of the aggregate such as size, grading, shape and distribution, the nominal maximum size of aggregates, and the nature of the asphalt mixture such as asphalt content, mix design and the void ratio [19–21]. Macrotexture mainly depends on the roughness of the road surface profile, controls the noise between tires and road surface as well as friction at high speeds, and mainly acts as drainage in rainy weather [22]. Microtexture refers to the fine structural irregularities on the surface of the aggregate particles, generally reaching the micrometer level, and is mainly related to the mineral composition of the aggregate particles [23]. Microtexture interacts with rubber tires at the molecular scale and provides adhesion, thus microtexture is important on both wet and dry pavements [24,25] and plays an important role in anti-slip [26].

Moretti [27] et al. conducted a lighting design and case study for continuously reinforced concrete pavement, plain concrete pavement, and asphalt pavement for the difference in pavement materials, the results showed that the total cost of cement pavement, energy consumption is 29% lower than that of asphalt pavement, and in the use of the period of 5 years, the plain concrete pavement consumes less and has a longer life span than the continuously reinforced cement pavement.

Due to the low accuracy of traditional pavement texture measurement in the past, Huang [28] and others independently developed a set of ultra-high-speed line laser testing systems based on the image recognition method, which can greatly improve the efficiency and accuracy of asphalt pavement structure, texture morphology three-dimensional data measurement. With the help of high-precision three-dimensional laser scanning technology, Yang et al [29,30] measured the surface texture characteristics of three typical grades of asphalt mixture specimens AC, SMA, and OGFC, according to the experimental data to establish a regression model with the mass ratio - the product of particle size and the average depth of the structure of the dependent variable, the model successfully predicted the pavement structure of asphalt specimen plate parameters of the different types of pavements. Weng et al [31] obtained the pavement texture data with the help of 3D laser scanning, extracted the surface trait parameters based on geometric features and the multi-scale feature parameters based on 2D wavelet transform as the model inputs, and predicted the gradation of asphalt under eight known gradations with the help of the model, and the goodness-of-fit was as high as 0.859. Viktoras [18] et al. considered that the brightness of pavement is related to the reflective properties of pavement, and different pavements can have different reflective properties. pavements can have different reflective properties depending on the surface texture, material and binder. Therefore, researchers conducted an experimental study on Vilnius city streets, which differed in color and age. The results show that red asphalt pavements have better reflective properties than black asphalt pavements. the simplified brightness factor of asphalt pavements installed in 2021 is about 12% lower than that of asphalt pavements installed 10 years ago.

To summarize, at present, few scholars have explored the light reflection characteristics of roads from the perspective of road surface topographic features and macro- and microstructures. Various studies are aimed at obtaining the reflection coefficient of pavement materials and analyzing the

 doi:10.20944/preprints202310.1535.v1

measurement uncertainty, but not enough research on the mechanism of the influence of material surface features on the reflection characteristics. The environmental factors involved in actual road lighting are more complicated, with various types of pavement materials and different three-dimensional morphology structures. Therefore, it is necessary to establish a scientific and reasonable quantitative expression model and choose a suitable and reliable optical research and design method to describe the law of road lighting in China.

Therefore, in this study, the LTL-XL Mark II retro-reflectometer and PATT-II pavement texture tester were used to obtain the retroreflection coefficient of asphalt mixtures and macro-micro-texture parameters both in the laboratory and on-site. In the labatory, the correlation between the retroreflection coefficient of asphalt mixtures and macro-micro-texture parameters before and after rutting test crushing was determined by measuring the retroreflection coefficient and macro-micro-texture parameters before and after the rutting test crushing, and a single-indicator impact model was established. The correlation between the macro-micro texture index and the retroreflection coefficient was determined by testing the relevant parameters in the field. A quantitative expression model of the retroreflection coefficient influenced by single and multiple texture parameters was established.

2. Materials and Methods

2.1. Asphalt mixtures

2.1.1. Asphalt

The binder used in the test was SBS-modified asphalt, according to the test protocol JTG E20-2011 [32]. The basic technical indicators of the asphalt test results are shown in Table 1. The results show that the technical indicators of the SBS-modified asphalt meet the specification requirements.

Table 1. Test results for SBS-modified asphalt.

Test Project	Unit	Technical Requirements	Test results	Test Method
Softening point (Universal method)	℃	≧55	61	JTG F40/T4507
Latency	（5℃,5 cm/min） cm	≧30	34	JTG F40/T4508
Needle penetration	（25℃） 1/10mm	60-80	69	JTG F40/4509
Needle penetration index (PI)	—	≧-0.4	-0.25	—
Flashpoint (open)	℃	≧230	280	JTG F40/T267
Solubility	%	≧99	99.6	JTG F40/T11148

2.1.2. Aggregates and fillers

Basalt was used as coarse aggregate and fine aggregate in the test, and limestone mineral powder was used as filler. According to the test specification JTG E42-2005[33], the density index of basalt is shown in Table 2, and the related technical index of limestone mineral powder is shown in Table 3. The results show that the aggregate and filler conformed to the specification JTG F40-2004 [34].

Preprints (www.preprints.org) | NOT PEER-REVIEWED | Posted: 24 October 2023 doi:10.20944/preprints202310.1535.v1

Table 2. Density of coarse and fine aggregates.

Coarse aggregate	Aggregate size	16–13.2	13.2–9.5	9.5 – 4.75	4.75–2.36	-
	Apparent relative density (g/cm³)	2.75	2.79	2.75	2.92	-
Fine aggregate	Aggregate size	2.36–1.18	1.18–0.6	0.6–0.3	0.3–0.15	0.15–0.075
	Apparent density (g/cm³)	2.87	2.86	2.82	2.79	2.98

Table 3. Limestone mineral powder technical index.

Sports event		Unit	stake a claim	Measurement results	Test Methods
Apparent density		g/cm³	≥2.50	2.524	T0352
Moisture content		-	≦1	0.3	T0103
Hydrophilicity			<1	0.66	T0353
Particle size range	<0.6mm	%	100	100	T0351
	<0.15mm	%	90-100	90.3	
	<0.075mm	%	75-100	74.6	
Exterior condition		-	No agglomeration	No agglomeration	-

Three graded asphalt mixtures of AC-13, SMA-13, and OGFC-13 were selected for the indoor test. The gradient curves are shown in **Figure 1.**

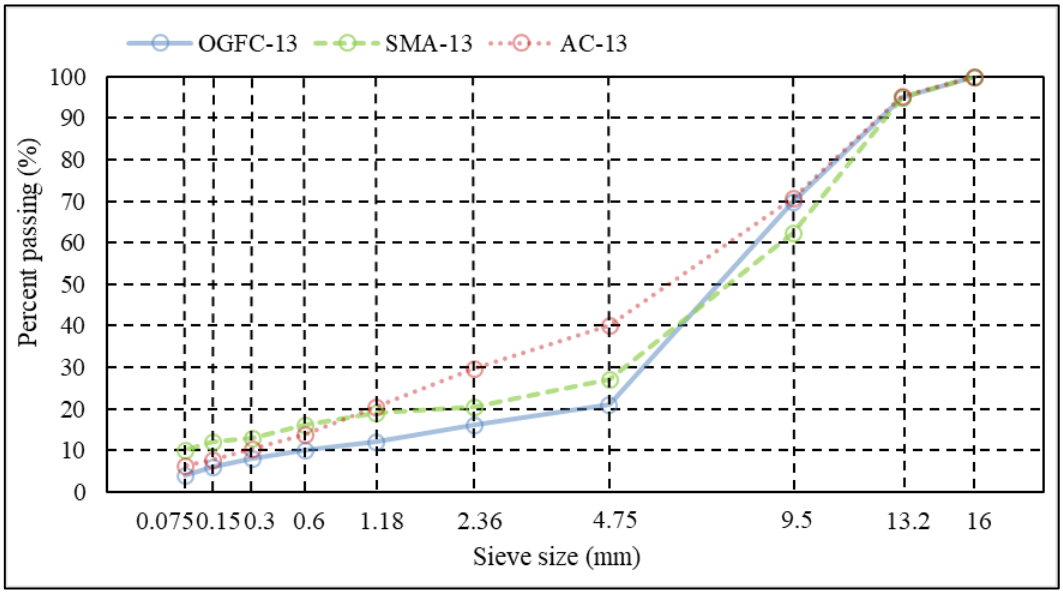

Figure 1. Grading curve.

2.1.3. Fibers

The blended fibers in the asphalt mixture of SMA-13 are lignin fibers, and their basic properties all meet the requirements of the JTG F40-2004 regulations [34]. Specific results are shown in Table 4.

Preprints (www.preprints.org) | NOT PEER-REVIEWED | Posted: 24 October 2023 doi:10.20944/preprints202310.1535.v1

Table 4. Basic properties of lignin fibers.

Pilot project	Unit	Technical requirement	Test results	Test Methods
Fiber length	mm	≤6	3.6	JTG/T533-2004
Ash content	%	18% ± 5, no volatiles	21.4	JTG/T533-2004
PH value	-	7.5±1.0	7.92	JTG/T533-2004
Oil absorption	%	≥5 times the fiber mass	846.2	JTG/T533-2004
Moisture content	%	≤5	3.2	JTG/T533-2004

2.2. Test methods

2.2.1. Rutting tests

This study is based on the test protocol JTG E20-2011 [32] for the rutting test. The test used a Hamburg rutting instrument HYCZ-5A, the test temperature is 60℃, the wheel pressure is 0.7 MPa, and the rutting specimen size is 300 mm × 300 mm × 50 mm. The test wheel is a solid tyre made of rubber, the outer diameter is 200 mm, the wheel width is 50 mm, the rubber layer thickness is 15 mm, the test wheel travels a distance of 230 mm ± 10 mm, the round-trip crushing speed is 42 times/min ± 1 time/min, the crushing time is 60 min, and the test process is shown in **Figure 2.**

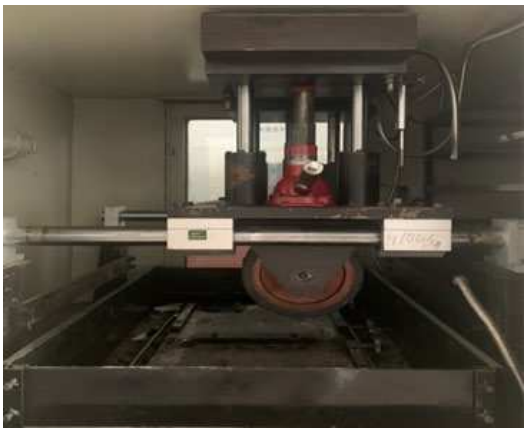

Figure 2. Rutting test.

2.2.2. Test of retroreflection coefficient of asphalt pavement

The research used an LTL-XL Mark II Retroreflectometer to test the retroreflectivity coefficient of the asphalt pavement RL. The RL value indicates the magnitude of the intensity of the reflected light from the pavement visible to the driver. The basic parameters of the retroreflectometer are listed in Table 5. To ensure the accuracy of the results, data collection was performed three times at adjacent positions of the same point, and the average value of the measured values was calculated by the device. The indoor and field testing processes are shown in **Figure 3.**

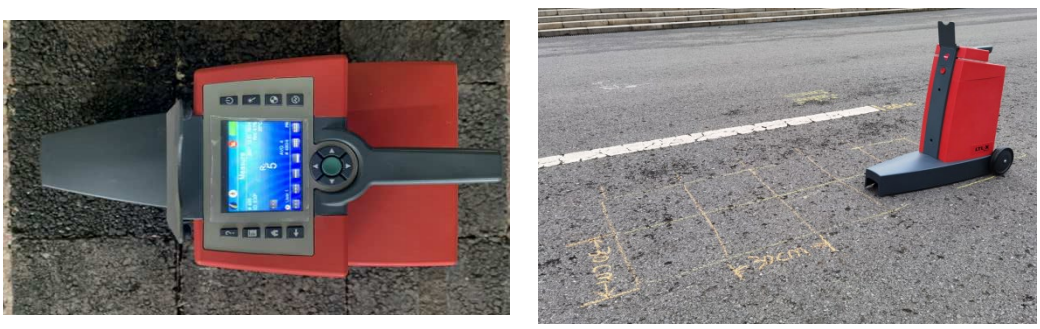

(**a**) (**b**)

Figure 3. Retroreflection coefficient test: (a) in-house testing and (b) field testing.

Preprints (www.preprints.org) | NOT PEER-REVIEWED | Posted: 24 October 2023 doi:10.20944/preprints202310.1535.v1

Table 5. Basic parameters of the retroreflective tester.

Sports event	Parameters
Measurement range	45 mm x 200 mm
The angle of incidence R_L	en 1436: 1.24° astm e 1710: 88.76°
Observation angle R_L	en 1436: 2.29° astm e 1710: 1.05°
R_L Scope	0 ~ 2000 mcd/(LX -m)2
Equipment length and width	Length: 573 mm Width: 222 mm
Equipment height	538 mm
Equipment weight	9.7 kg
Operating temperature	0℃~45℃

2.2.3. Testing of Asphalt Pavement Texture Parameters

In this study, we used the PATT-II pavement antislip texture tester to obtain asphalt pavement texture information. The scanning parameters of the tester's laser sensor are shown in Table 6. At the retroreflection coefficient measurement point, the macro- and microtexture indices of indoor rutted slabs or asphalt pavements in the field were measured using the Pavement Antiskid Texture Tester, as shown in Figure 4.

(**a**) (**b**)

Figure 4. Pavement texture index test: (a) in-house testing,(b) Field testing.

Table 6. Scanning parameters of the laser sensor.

Sports event	Parameters
Scan length	40 ~ 300 mm
Scanning width	20 ~ 300 mm
Travel step	Integer multiple of scan width
Absolute height from the scanned specimen	80 mm

3. Results and Discussion

3.1. Effect of texture index on light reflection characteristics of asphalt mixture specimens before and after rutting and crushing

To study the optical reflection characteristics of the asphalt mixtures, we used three grades of asphalt mixtures, AC-13, SMA-13, and OGFC-13, to conduct indoor rutting tests to simulate the crushing action of the wheels on the roadway. The macroscopic and microscopic texture indices and retro-reflection coefficients before and after the crushing of various rutted specimens were then measured to analyze the effect of the texture indices of the asphalt mixtures on the optical reflection characteristics in the indoor tests.

3.1.1. Analysis of Pavement Texture Parameters

According to the relevant research results, seven texture parameters, namely, macrotexture surface area S_1, microtexture surface area S_2, macrotexture distribution density D_1, microtexture

Preprints (www.preprints.org) | NOT PEER-REVIEWED | Posted: 24 October 2023 doi:10.20944/preprints202310.1535.v1

distribution density D_2, profile slope root-mean-square Δq, skewness R_{sk}, and kurtosis R_{ku} of asphalt mixture specimens before and after crushing in the rutting test were selected for comparative analysis. The specific measurement results are shown in **Figure 5**.

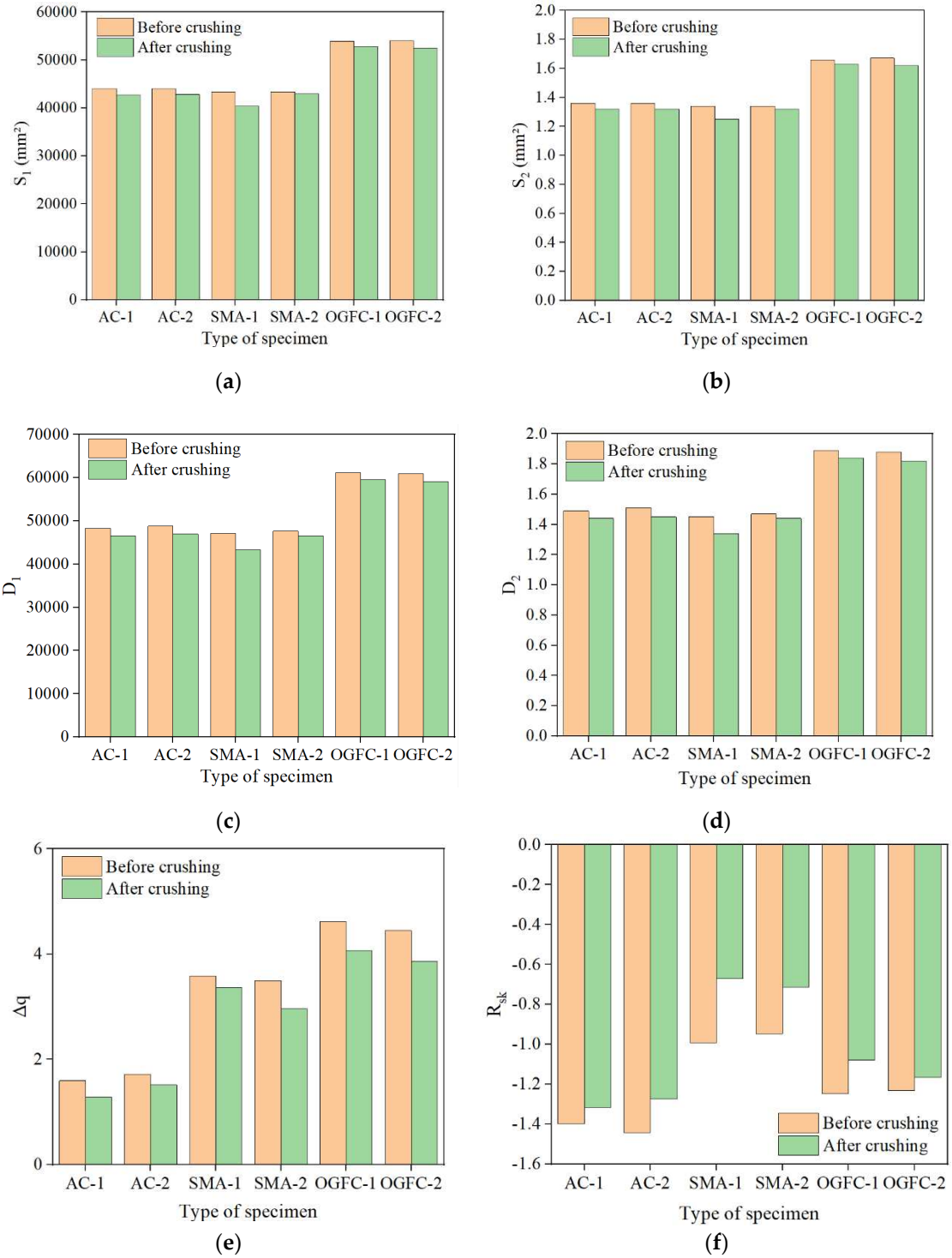

Preprints (www.preprints.org) | NOT PEER-REVIEWED | Posted: 24 October 2023 doi:10.20944/preprints202310.1535.v1

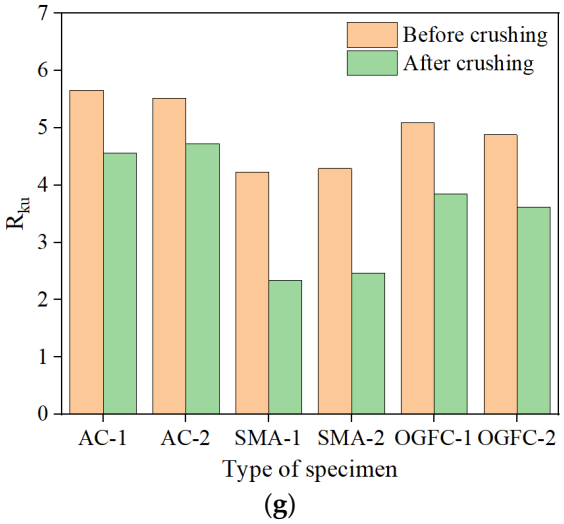

Figure 5. Comparison of texture parameters of different types of rutted specimens before and after crushing in rutting test: (a) Macrotexture surface area comparison, (b) microtexture surface area comparison, (c) macroscopic texture distribution density, (d) microscopic texture, (e) profile slope root mean square, (f) skewness comparison, and (g) kurtosis comparison.

Figure 5 shows that S_1, S_2, D_1, D_2, Δq, R_{ku} of the asphalt mixture specimens with AC, SMA, and OGFC gradations after crushing in the rutting test decreased and Rsk increased. This may be because the surface of the asphalt mixture becomes flatter at the rutting location after crushing by the rutting meter, resulting in corresponding changes in the different texture parameters.

Figure 5(a) – (e) show that S_1, S_2, D_1, D_2, Δq before and after the rutting test of AC- and SMA-graded asphalt mixture specimens are smaller than those of the OGFC-graded asphalt mixture. This is mainly related to the gradation design of the asphalt mixture. The OGFC-type asphalt mixture is a typical open-graded mixture with a large proportion of coarse aggregates, a large void ratio, and prominent morphology, which has a greater difference in surface texture than AC and SMA. The surface texture of the Type A asphalt mixtures exhibits greater variability. Before and after rutting test milling, the S_1, S_2, D_1, and D_2 values of the two types of rutted specimens, AC and SMA, were relatively similar, and the changing trend of different texture indices before and after milling was consistent. Analyzing **Figure 5** (f) and (g), it can be seen that AC < OGFC < SMA in terms of skewness index R_{sk}, and SMA < OGFC < AC in terms of kurtosis index R_{ku}.

3.1.2. Analysis of retroreflection coefficient measurement results

Using the retroreflection coefficient to characterize the light reflection properties of the asphalt mixture specimens, the reverse reflection coefficients of different gradation types of asphalt mixtures before and after crushing by the rutting test were comparatively analyzed. Specific results are shown in **Figure 6**.

Preprints (www.preprints.org) | NOT PEER-REVIEWED | Posted: 24 October 2023 doi:10.20944/preprints202310.1535.v1

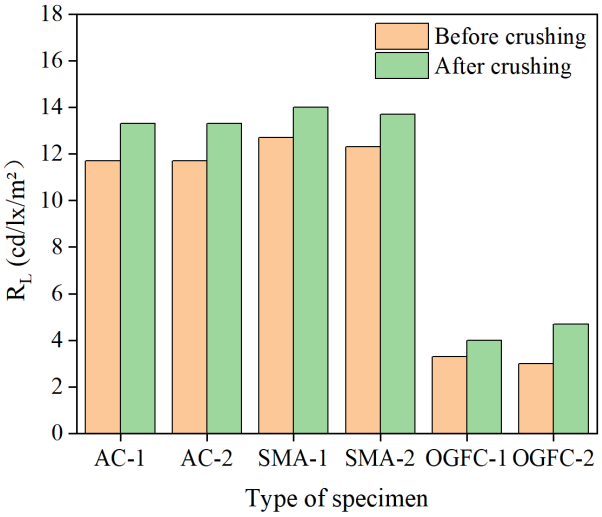

Figure 6. Reverse reflection coefficients of different types of rutted specimens before and after crushing.

As shown in **Figure 6**, the reverse reflection coefficients at the rutted locations of the three types of rutted specimens, AC, SMA, and OGFC, were all larger than the reverse reflection coefficients. This may be because after the rutting instrument is rolled, the location becomes dense, and the asphalt mixture morphology changes accordingly. When measured by the instrument, the light reflection of the surface is more similar to the specular reflection than the rough surface that has not been rolled, and the intensity of the reflected light increases, and the measured retroreflection coefficient also increases.

Meanwhile, it can be found that the reverse reflection coefficients of the AC and SMA rutted specimens before and after crushing are similar; the reason may be that the surface area of the macro-micro texture and the density of macro-micro texture distribution of the AC and SMA rutted specimens are close to each other; and the reverse reflection coefficients of AC and SMA rutted specimens before and after crushing are greater than those of OGFC, which may be because a larger proportion of coarse aggregates is used in the preparation of OGFC rutted specimens. The reason may be that a larger proportion of coarse aggregate was used in the preparation of OGFC rutted specimens, and the texture distribution of the surface is wider and the pores are larger, so that the light reflection on the surface is closer to diffuse reflection, the intensity of the reflected light is smaller, and the measured retroreflection coefficient is smaller.

3.1.3. Influence of Asphalt Pavement Texture Parameters on the Coefficient of Retroreflection

To analyze the effect of asphalt mixture surface texture index on optical reflection characteristics, macro- and microtexture indices before and after specimen rutting test milling were established using the retroreflection coefficient R_L, a quadratic polynomial functional relationship equation, to analyze the effect of individual texture index factors on optical reflection characteristics. Specific results are shown in **Figure 7.**

Preprints (www.preprints.org) | NOT PEER-REVIEWED | Posted: 24 October 2023 doi:10.20944/preprints202310.1535.v1

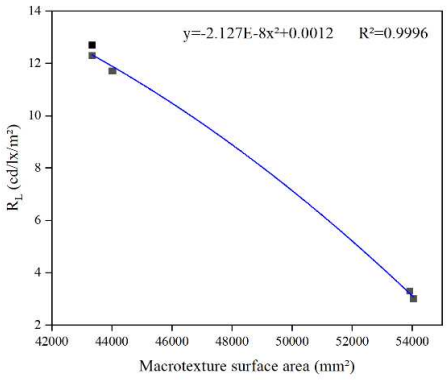

(a1)

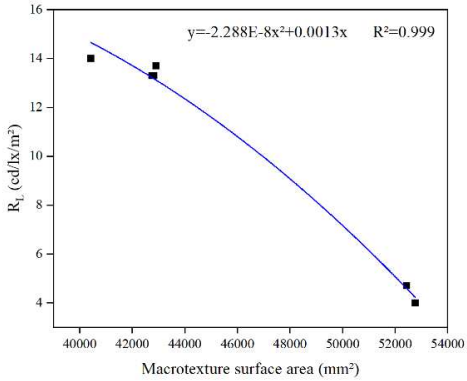

(a2)

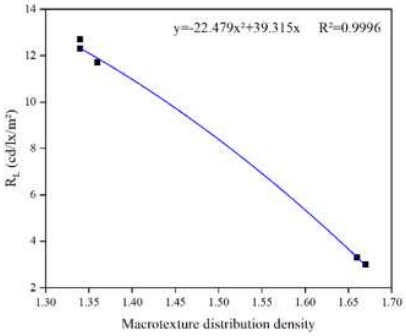

(b1)

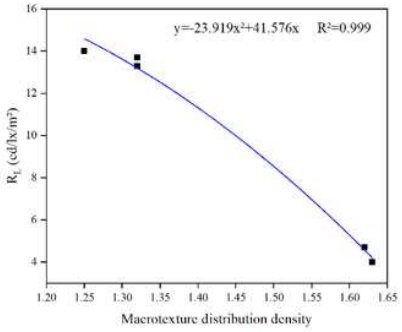

(b2)

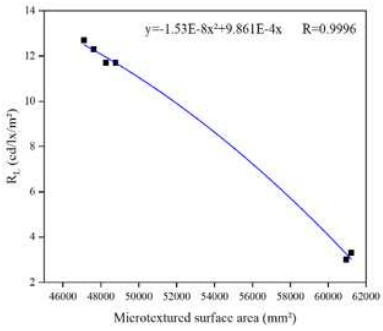

(c1)

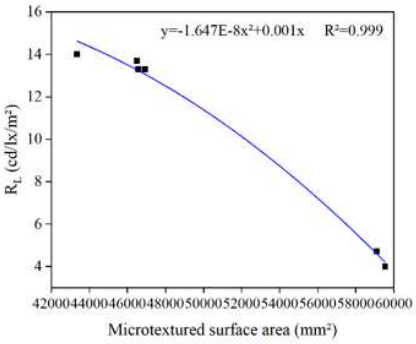

(c2)

Preprints (www.preprints.org) | NOT PEER-REVIEWED | Posted: 24 October 2023 doi:10.20944/preprints202310.1535.v1

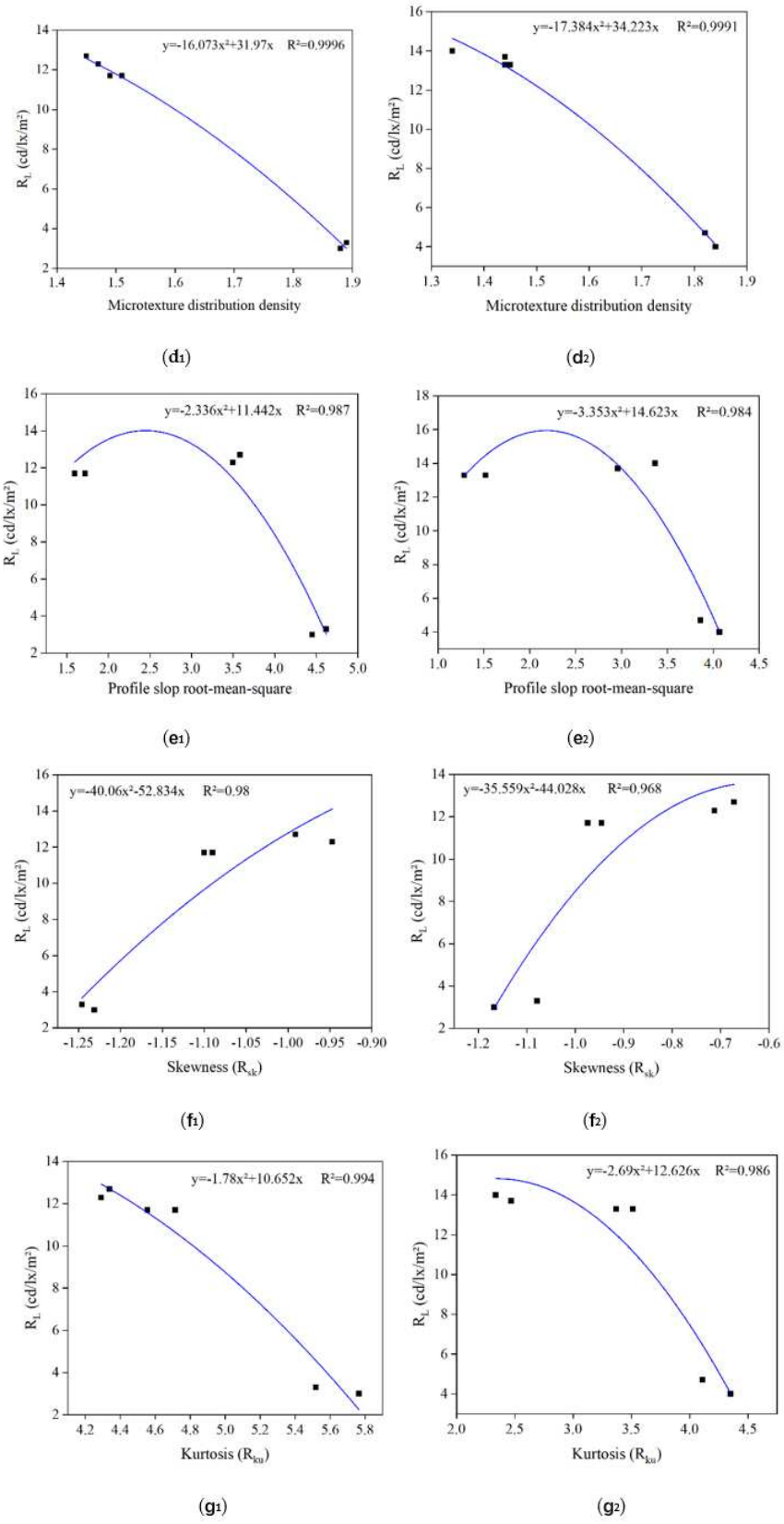

Figure 7. Model of the correspondence between the retroreflection coefficient R_L and the texture index before and after crushing: (a_1) Rutted specimen S1 before crushing is correlated with RL, (a_2) Rutted specimen S_1 after crushing is correlated with RL, (b_1) Rutted specimen D_1 before crushing is related to R_L, (b_2) Rutted specimen D_1 after crushing is related to R_L, (c_1) Rutted specimen before crushing S_2 Correlation with R_L, (c_2) Rutted specimen after crushing S_2 Correlation with RL, (D_1) Rutted specimen D_2 before crushing correlates with R_L, (d_2) Rutted specimen D_2 after crushing correlates with RL, (e_1)

Preprints (www.preprints.org) | NOT PEER-REVIEWED | Posted: 24 October 2023 doi:10.20944/preprints202310.1535.v1

Correlation between Δq and R_L for rutted specimens before crushing, (e_2) Correlation between Δq and R_L for rutted specimens after crushing, (f_1) Pre-crush rutted specimen R_{sk} correlates with R_L, (f_2) Post-crush rutted specimen R_{sk} correlates with R_L, (g_1) Correlation between R_{ku} and R_L for rutted specimens before crushing, (g_2) Correlation between R_{ku} and R_L for rutted specimens after crushing.

As can be seen from **Figure 7**, the macrotexture surface area S_1, microtexture surface area S_2, macrotexture distribution density D_1, microtexture distribution density D_2, profile slope root-mean-square Δq, skewness R_{sk}, and kurtosis R_{ku} of asphalt mixture specimens before and after crushing in the rutting test were correlated with the retroreflection coefficient R_L as a quadratic polynomial function with a better fitting effect, and the R_2 was above 0.95.

3.2. Optical Reflection Characterization of Field Asphalt Pavements Based on Texture Parameters

To further study the influence mechanism of asphalt pavement texture parameters on optical reflection characteristics, eight on-site asphalt roads were tested using a retroreflection coefficient measuring instrument and pavement texture tester. Correlation equations between texture indices and optical reflection characteristics were constructed to analyze the relationship between the influence of macroscopic and microscopic texture indices on the reverse reflection coefficient.

3.2.1. Modeling of the influence of single texture index factors on light reflection characteristics

Considering the functional relationship between the texture index and the retroreflection coefficient of asphalt mixture specimens before and after the indoor rutting test, based on the macroscopic and microscopic texture parameters and retroreflection coefficient obtained from the eight on-site asphalt pavements, a quadratic polynomial relationship model between individual texture parameters and retroreflection coefficients was constructed to analyze the effect of individual texture index factors on the light reflectance characteristics. Specific results are shown in **Figure 8.**

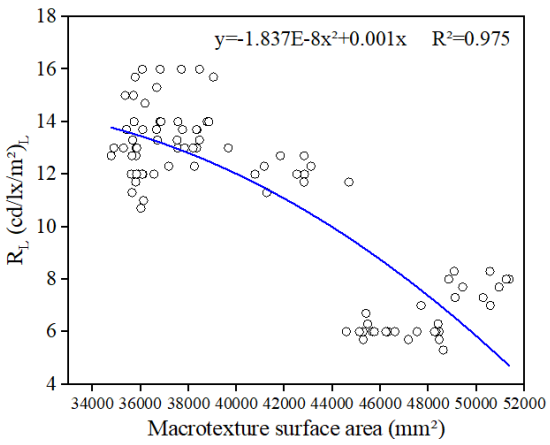

(**a**)

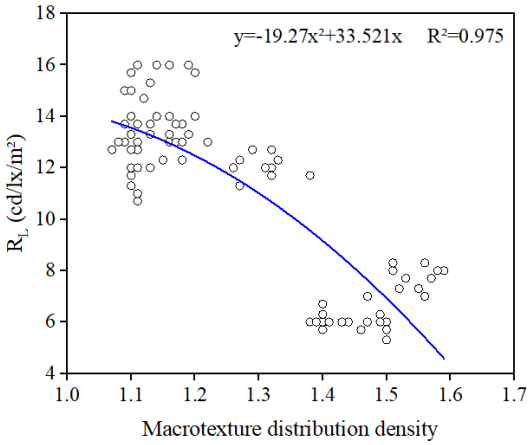

(**b**)

Preprints (www.preprints.org) | NOT PEER-REVIEWED | Posted: 24 October 2023 doi:10.20944/preprints202310.1535.v1

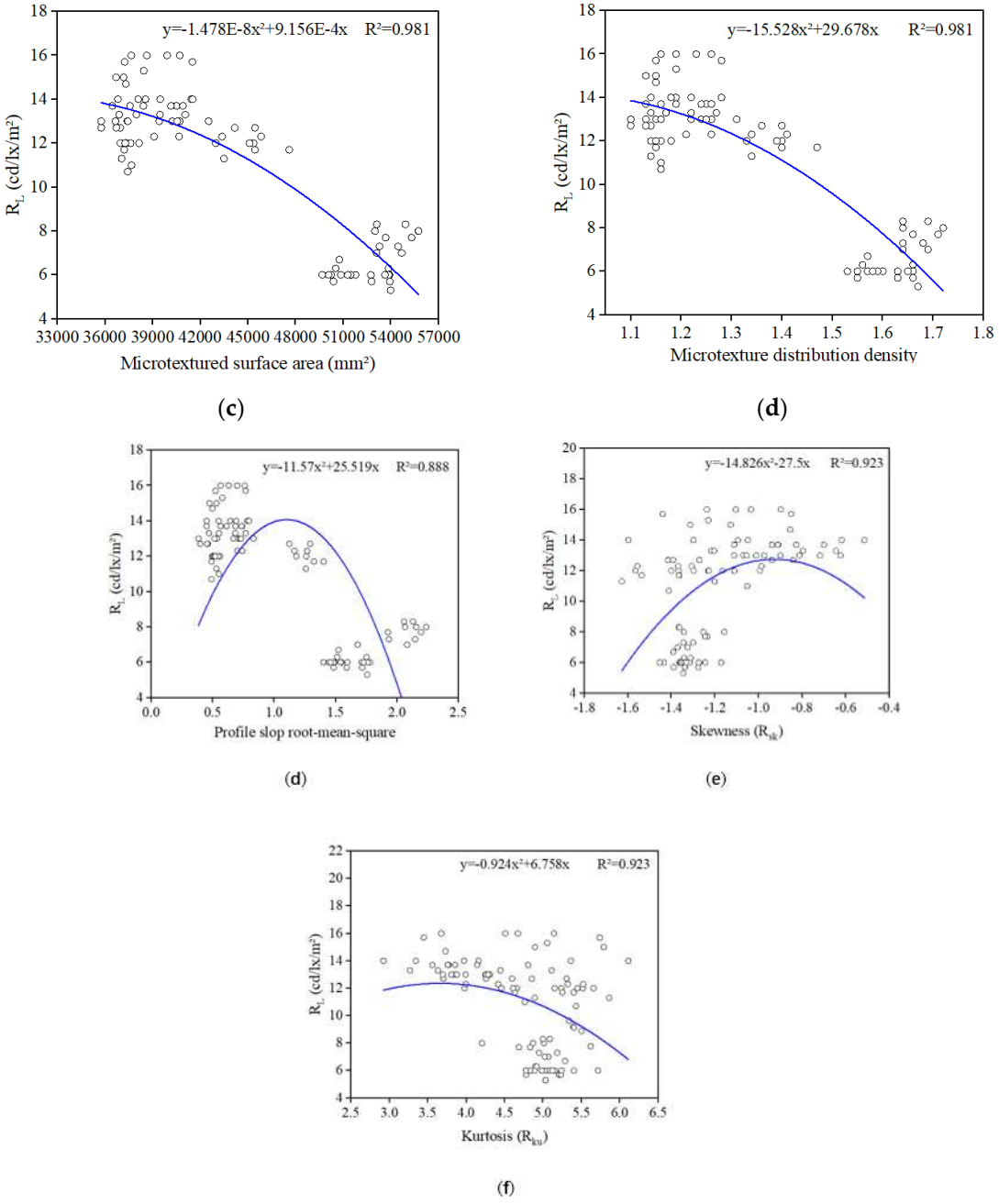

Figure 8. One-factor modeling of pavement texture index and reverse reflection coefficient: (a) S_1 correlates with R_L, (b) D_1 correlates with R_L,(c) S_2 correlates with R_L, (d) D_2 correlates with R_L,(e) Δq correlates with R_L, (f) R_{sk} correlates with R_L,(g) R_{ku} correlates with R_L.

Figure 8 shows that the macro-texture surface area S_1, microtexture surface area S_2, macro-texture distribution density D_1, microtexture distribution density D_2, profile slope root-mean-square Δq, skewness R_{sk}, and kurtosis R_{ku} of a series of macroscopic and microscopic texture parameters of the actual asphalt pavement and retroreflection coefficient R_L are all quadratic polynomial correlations, and the constructed single-factor influence model's R^2 reaches more than 0.90. The results show that the retroreflection coefficient can be effectively predicted on the basis of the texture parameters of asphalt pavements. Among them, the correlation models of S_1, S_2, D_1, D_2, and R_L all have R^2 above 0.95, which are effective in predicting the light reflection characteristics.

3.2.2. Modeling of the influence of multitexture index factors on light reflection characteristics

Preprints (www.preprints.org) | NOT PEER-REVIEWED | Posted: 24 October 2023 doi:10.20944/preprints202310.1535.v1

To further investigate the influence of asphalt pavement texture indexes on the reverse reflection coefficient, this study deeply analyzes and mines all the macro- and microtexture parameters and reverse reflection coefficients collected from asphalt pavements in the field and the retroreflection coefficient R_L with the help of Weka software, and constructs a linear and nonlinear model between the two. When the absolute value of the correlation coefficient is greater than or equal to 0.8, it can be considered that the linear correlation between the two variables is high.

3.2.2.1. Linear models

After the seven texture metrics were cross-validated several times using Weka software, it was determined that the model had the highest correlation and the smallest error when the three metrics, namely, profile slope root-mean-square Δq, the skewness R_{sk}, and kurtosis R_{ku}, were used for the multifactor linear modeling. The quantitative expression of the multifactor linear model is shown in Eq. 1, which has a correlation coefficient of 0.8393, a mean error value of 1.543, and a profile slope root mean square of 1.8132. The linear correlation between variables can be considered to be high when the absolute value of the correlation coefficient is greater than or equal to 0.8. The results show that the prediction accuracy of the model is high, and the correlation between the texture index and R_L is good.

$$R_L = -5.3671\Delta q - 6.7798R_{sk} - 2.664R_{ku} + 21.1746 \quad (1)$$

3.2.2.2. Non-Linear Models

In this section, the multilayer perceptron model based on the B-P algorithm is used to construct a nonlinear model of the effect of the asphalt pavement macro- and microtexture parameters on the reverse reflection coefficient. The relationships between the input and hidden layers in the model established in this experiment are shown in **Figure 9**. The model is obtained by regression using the multilayer perceptron module of Weka software, in which S_1, S_2, D_1, D_2, Δq, R_{sk}, and R_{ku} are the input layers. There is one layer of the hidden layer, and the number of nodes in the hidden layer is four: Nodes 1, 2, 3, and Node4. The neurons in the hidden layer use the sigmoid activation function, and its mapping relationship is given by Eq. 2. The output layer is R_L.

$$f(x) = \frac{1}{1+e^{-x}} \quad (2)$$

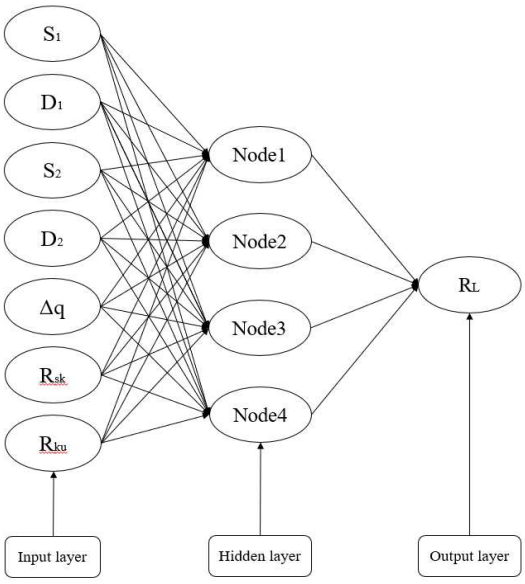

Figure 9. Multilayer perceptron model.

Preprints (www.preprints.org) | NOT PEER-REVIEWED | Posted: 24 October 2023 doi:10.20944/preprints202310.1535.v1

The analysis shows that the weight relationship between the input layer and the hidden layer and the weight relationship between the hidden layer and the output layer are shown in Tables 7 and 8. The output results of the multifactor nonlinear model show that the correlation coefficient between the texture parameters and the R_L coefficient is 0.9191, the average error value is 1.0404, and the root-mean-square error is 1.3342, which indicates that the seven parameters, S_1, D_1, S_2, D_2, Δq, R_{sk}, and R_{ku}, are better correlated with R_L and that the nonlinear model has a higher prediction accuracy than the linear model.

Table 7. Weight relationship between the input and hidden layers.

Weights	Node1	Node2	Node3	Node4
S1	0.576	0.249	0.121	-0.842
D1	0.597	0.417	0.077	-0.717
S2	-1.419	-2.567	-0.171	-1.113
D2	-1.666	-2.382	-0.184	-0.735
Δq	3.638	0.794	0.557	-1.227
Rsk	-0.154	0.395	0.267	0.285
Rku	-1.409	-0.367	-0.198	0.028

Table 8. Weighting relationship between the hiding and output layers.

Weights	R_L
Node1	0.856
Node2	1.893
Node3	0.095
Node4	-0.977

4. Conclusion

In this study, the macroscopic texture index and retroreflection coefficient of indoor rutted specimens and field asphalt pavements were measured, and the correlation between the macroscopic texture index and retroreflection coefficient was determined. Then, single- and multifactor models of the influence of the macroscopic texture index on the optical reflection characteristics of asphalt pavements were constructed. The main conclusions were as follows：

- Changes in texture parameters and light reflection properties before and after the indoor rutting test were compared. After the rutting test, S_1, S_2, D_1, D_2, Δq, and R_{ku} of the different graded asphalt mixture specimens decreased, R_{sk} increased, and R_L tended to increase. S_1, S_2, D_1, D_2, and Δq of AC and SMA-graded specimens before and after the rutting test were smaller than those of the OGFC-graded asphalt mixture, and R_L was much larger than that of OGFC-graded specimens.
- Relationship equations between the texture indices and reverse reflection coefficients of the indoor asphalt mixture specimens were established. The individual macro and micro texture parameters, including S_1, S_2, D_1, D_2, Δq, R_{sk}, and R_{ku} of asphalt mixture specimens before and after crushing in the rutting test, showed a quadratic polynomial influence on the retroreflection coefficient R_L, which was a good fit.
- The results of the one-factor modeling of the light reflection characteristics by texture metrics of asphalt pavements in the field showed a good quadratic multinomial expression relationship between single macro and micro texture metrics and the retro-reflection coefficient R_L. The correlation coefficient of the multifactor influence model is 0.8393 for the linear model and 0.9191 for the nonlinear model, and the nonlinear model based on texture parameters can improve the prediction accuracy of the reverse reflection coefficient.

Author Contributions: Conceptualization, P.X.; methodology, G.Q.; validation, C.Z.; formal analysis, X.W.; investigation, H.Y.; resources, P.X.; data curation, C.Z.; writing—original draft preparation, P.X.; writing—review and editing, H.Z.; visualization, C.Z.; supervision, G.Q.; project administration, P.X.; funding acquisition, P.X. All authors have read and agreed to the published version of the manuscript.

Funding: This research was funded by the National Key Research and Development Program of China, grant number 2022YFB2601900, the National Natural Science Foundation of China, grant number 52227815, and the Open Fund of Hunan Key Laboratory of Smart Roadway and Cooperative Vehicle-Infrastructure Systems (Changsha University of Science & Technology, grant number: kfj210701)

Institutional Review Board Statement: Not applicable.

Informed Consent Statement: Not applicable.

Data Availability Statement: Not applicable.

Conflicts of Interest: The authors declare no conflict of interest.

References

1. Box, P. C.; Alroth, W. Relationship between illumination and freeway accidents; **1970**. pp 85-67.
2. Elvik, R., Meta-analysis of evaluations of public lighting as accident countermeasure. *Transportation Research Record* **1995,** 1485, (1), 12-24.
3. Elvik, R.; Høye, A.; Vaa, T.; Sørensen, M., *The handbook of road safety measures*. Emerald Group Publishing Limited: **2009**.
4. Gidlund, H.; Lindgren, M.; Muzet, V.; Rossi, G.; Iacomussi, P., Road surface photometric characterisation and its impact on energy savings. *Coatings* **2019,** 9, (5), 286.
5. CIE 144:2001 Road Surface and Road Marking Reflection Characteristics. *International Commission on Illumination (CIE)*: Vienna,Austria, **2001.**
6. Greffier, F.; Muzet, V.; Boucher, V.; Fournela, F.; Lebouc, L.; Liandrat, S., Influence of pavement heterogeneity and observation angle on lighting design: Study with new metrics. *Sustainability* **2021,** 13, (21), 11789.
7. Ogando-Martínez, A.; Troncoso-Pastoriza, F.; Granada-Álvarez, E.; Eguía-Oller, P., Ellipsoid-based approximation method for the estimation of the actual reduced luminance coefficients of road surfaces for accurate lighting simulations. *Sustainable Cities and Society* **2020,** 63, 102502.
8. Muzet, V.; Greffier, F.; Verny, P., Optimization of road surface reflections properties and lighting: learning of a three-year experiment. *29th Quadrennial Session of the CIE* **2019**, 525-535.
9. Galatanu, C. D.; Canale, L., Measuring Reduced Luminance Coefficients for Asphalt Based on Imaging Method. *2022 IEEE International Conference on Environment and Electrical Engineering and 2022 IEEE Industrial and Commercial Power Systems Europe (EEEIC / I&CPS Europe)* **2022**, 1-5.
10. Li, W.; Hu, Y.; Ji, Y.; Liu, M.; Shen, H., A Database Retrieval Method for the Prediction of Reduced Luminance Coefficient Tables of A Road Surface Based on Measurements in Situ. *LEUKOS* **2020,** 18, 21 – 29.
11. Florian, G.; Valérie, M.; Gautier, M.; Paul, V.; Patrick, T. Design of an adaptive lighting system able to consider the evolution of pavement reflection properties according to their moisture state, *2021 Joint Conference-11th International Conference on Energy Efficiency in Domestic Appliances and Lighting & 17th International Symposium on the Science and Technology of Lighting (EEDAL/LS: 17)*, 2022; IEEE: 2022; pp 1-6.
12. Muzet, V.; Bernasconi, J.; Iacomussi, P.; Liandrat, S.; Greffier, F.; Blattner, P.; Reber, J.; Lindgren, M., Review of road surface photometry methods and devices–Proposal for new measurement geometries. *Lighting Research & Technology* **2021,** 53, (3), 213-229.
13. Chen, X.; Zheng, X.; Wu, C., Portable instrument to measure the average luminance coefficient of a road surface. *Measurement Science and Technology* **2014,** 25, (3), 035203.
14. Saint-Jacques, E.; Dumont, E.; Villa, C. Characterisation of the reflection properties of road surfaces using an in-lab gonioreflectometer, Proceedings of the CIE 2017 Midterm Meetings and Conference on Smarter Lighting for Better Life, *International Commission on Illumination*, CIE, Jeju Island, Korea, 2017; **2017**; pp 23-25.
15. Hall, J. W.; Smith, K. L.; Titus-Glover, L.; Evans, L. D.; Wambold, J. C.; Yager, T. J., Guide for Pavement Friction Contractor's Final Report for National Cooperative Highway Research Program (NCHRP) Project 01-43. *Transportation Research Board of the National Academies, Washington, D.C* **2009**.
16. Association, P. W. R. Road safety manual: Route market; **2003**.
17. Honghui, L.; Sen, H.; Bo, L., Foreign asphalt pavement coarse structure test method and application. *Journal of China and Foreign Highway* **2009**, 29, (2), 66-68.
18. Lunkevičiūtė, D.; Vorobjovas, V.; Vitta, P.; Čygas, D., Research of the Luminance of Asphalt Pavements in Trafficked Areas. *Sustainability* **2023,** 15, (3), 2826.
19. Kogbara, R. B.; Masad, E. A.; Kassem, E.; Scarpas, A.; Anupam, K., A state-of-the-art review of parameters influencing measurement and modeling of skid resistance of asphalt pavements. *Constr Build Mater* **2016,** 114, 602-617.
20. Chao, Z.; Huanan, Y.; Xuan, Z.; Ding, Y.; Xinghai, P.; Xianpeng, F., Unified characterization of rubber asphalt mixture strength under different stress loading paths. *J Mater Civil Eng* **2023**.

21. Huanan, Y.; Chao, Z.; Guoping, Q.; Jinguo, G.; Xuan, Z.; Ding, Y.; Changyun, S., Characterization and evaluation of coarse aggregate wearing morphology on mechanical properties of asphalt mixture. *Constr Build Mater* **2023**, 388, 131299.
22. Siqi, W. Research on digitization technology of asphalt pavement surface texture. *Southeast University*, **2016**.
23. Masad, E.; Rezaei, A.; Chowdhury, A., Field Evaluation of Asphalt Mixture Skid Resistance and Its Relationship to Aggregate Characteristics. *Asphalt Mixtures* **2011**.
24. Dunford, A. Friction and the texture of aggregate particles used in the road surface course. *University of Nottingham*, **2013**.
25. Flintsch, G. W.; McGhee, K. K.; Najafi, S.; León, I. E. d., The Little Book of Tire Pavement Friction. *Surface Properties Consortium*. **2012**, 0-22.
26. Mcquaid, G.; Woodward, D.; Millar, P.; Friel, S. In *Use of Close Range Photogrammetry to assess the microtexture of asphalt surfacing aggregates*, Proceedings of the International Journal of Pavements Conference - Maintenance and Rehabilitation of Pavements and Technological Control, 2013; **2013**.
27. Moretti, L.; Cantisani, G.; Di Mascio, P.; Caro, S., Technical and economic evaluation of lighting and pavement in Italian road tunnels. *Tunnelling and Underground Space Technology* **2017,** 65, 42-52
28. Zhiyong, H.; Bo, C.; Weixiong, L.; Xiaoning, Z.; Fuda, C., Line Laser Measurement Methods and Depth of Construction of Asphalt Pavements. *Science Technology and Engineering* **2019**, 19, (23), 252-258.
29. Enhui, Y.; Qiang, C.; Jie, L.; Haibo, D.; Bing, H.; Yanjun, Q., Surface Texture Reconstruction and Construction Depth Prediction Model for Asphalt Pavements. *China Journal of Highway and Transpor* **2023**, 36, (6), 14.
30. Shihai, D.; Enhui, Y.; Chenping, W.; Yaying, J.; Kaiyun, L.; Xinrui, Z., Three-dimensional high-precision laser non-contact inspection of asphalt pavement surface texture. *Journal of Southwest JiaoTong Universit* **2020**, 55, (4), 758-764.
31. Zihang, W., Asphalt pavement gradation prediction method based on three-dimensional texture characteristics. *Journal of Tongji University(Natural Science)* **2022**, 50, (6), 879-890.
32. *JTG E20-2011*; Bitumen and Bituminous Mixtures for Highway Engineering. Ministry of Transport of the People's Republic of China: Beijing, China, 2011.
33. *JTG E42-2005*; Test Methods of Aggregate for Highway Engineering. Ministry of Transport of the People's Republic of China: Beijing, China, 2005.
34. *JTG F40-2004;* Technical Specifications for Construction of Highway Asphalt Pavements. Ministry of Transport of the People's Republic of China: Beijing, China, 2004.